Theoretical Approach to the Wear and Tear Mechanism in Triosephoshate Isomerase: A QM/MM Study

F. A. S. Konuklar,[†] V. Aviyente,*[,†] G. Monard,[‡] and M. F. Ruiz Lopez[‡]

Boğaziçi University, Department of Chemistry, 34342 Bebek-Istanbul, Turkey, and Groupe de Chimie et Biochimie Théorique, UMR CNRS-UHP No. 7565, Université Henri Poincaré-Nancy I, 54506 Vandoeuvre-les-Nancy, France

Received: December 10, 2003

The relationship between the deamidation mechanism and the catalytic activity of triosephoshate isomerase has been studied with a QM/MM method where AM1/AMBER parametrization was used. The mechanism considered in this study is compared to that previously described for a dipeptide model in vacuum using density functional theory. The present study focuses on determining whether the ligand-induced deamidation proceeds via an intrasubunit or intersubunit transmission of the conformational change. Our calculations have shown that, although the binding of the substrate has an effect on the conformational preferences of asparagine 15 on the same subunit, deamidation takes place on the juxtaposed subunit.

Introduction

Triosephosphate isomerase (TIM) is a homodimeric enzyme that rapidly and reversibly converts dihydroxyacetone phosphate (DHAP) into glyceraldehyde-3-phosphate (GAP) in the glycolytic pathway. It is a simple enzyme that requires no coenzyme or any cofactor during processing and can be categorized as a perfect enzyme because the reaction rate is dependent only on the rate of diffusion of the substrate. The structural changes that occur during catalytic activity as well as the thermodynamics and kinetics of the enzyme have already been intensively studied.[1−14]

Conformational changes in proteins are often an essential part of the enzyme mechanisms. Considered to be nonregular elements of protein secondary structure, loops are variable in size and sequence and trace a curved path through space. TIM possesses an intriguing flexible loop that appears to be close to the active site when the substrate binds by interacting with the peripheral phosphate oxygen atoms of the ligand in the active site.[8,9] Joseph et al.[8] have combined molecular dynamics (MD) simulations with structural and sequence data to obtain a description of the so-called "loop transition" in the TIM enzyme. Each subunit contains a loop region (residues 166 to 176) that projects into solvent in the unliganded enzyme and closes over the active site when the substrate binds (Figure 1). An 11-residue loop region moves more than 7 Å and closes over the active site when the substrate binds, and a hinge-type motion takes place. There are no large main-chain energy barriers between the open and closed forms. Pompliano et al.[9] have found that the loop is essential to the catalysis because it protects the active site from contact with bulk water. ^{31}P NMR studies by Schanekerz et al.[10] have shown that the two catalytic centers act completely independently of each other.

Deamidation is one of the spontaneous degradation reactions limiting the lifetime of proteins.[15−19] It occurs both in vitro (e.g., during the isolation and storage of proteins) and in vivo during the development and/or aging of cells. Deamidation is a hydrolytic reaction resulting not only in the introduction of negative charges but also in a change of the primary structure, which in turn may affect the secondary and tertiary structures of proteins or peptides. These changes in the structure and charge of proteins may affect their biological activity, which is especially important in aging organisms, where deamidated forms are accumulated. TIM from mammals undergoes specific deamidation at asparagines 15 and 71 on each subunit of the dimeric protein[20−26] (Figure 1). The presence of a glycine (Gly) residue next to asparagine (Asn) is necessary for a deamidation reaction to take place. One unique property of Gly is the flexibility that is imparted to the peptide main chain. Glycine-containing peptides can adopt conformations favorable to the reaction as compared to peptides where the presence of a β-side-chain carbon restricts the range of motion. Indeed, the deamidating sites in TIM consist of an Asn-Gly dipeptide unit. Mechanistic studies have suggested that the reaction at neutral and basic pH is intramolecular and proceeds through a five-membered succinimide intermediate (Figure 2).[27] This intermediate is formed via a nucleophilic attack on the side-chain carbonyl carbon of Asn by the backbone nitrogen of the ensuing amino acid residue, releasing ammonia.[27] The deamidation at the dimer interface initiates subunit dissociation, unfolding, and protein degradation.

Sun et al.[23] have studied the effects of active-site modification and deamidation on the structure of the enzyme as reflected by the susceptibility of the enzyme to denaturation and proteolysis. The site of the primary deamidation has been shown to be Asn_{71}, with the secondary deamidation occurring at Asn_{15} ($<$0.5 nm away on the neighboring subunit). The deamidation introduces two pairs of negative charges into the subunit interface. These negative charges initiate subunit dissociation and unfolding and lead to proteolytic degradation.

In 1994, Ramos-Garza et al.[24] studied the effect of water on TIM catalysis and deamidation. They showed that as the rate of catalysis is diminished by lowering the water concentration, deamidation per catalytic cycle is increased. However, for very low water concentration, at which catalysis is hardly detectable,

* Corresponding author. E-mail: aviye@boun.edu.tr.
[†] Boğaziçi University.
[‡] Université Henri Poincaré-Nancy I.

10.1021/jp037791m CCC: $27.50
Published on Web 03/02/2004

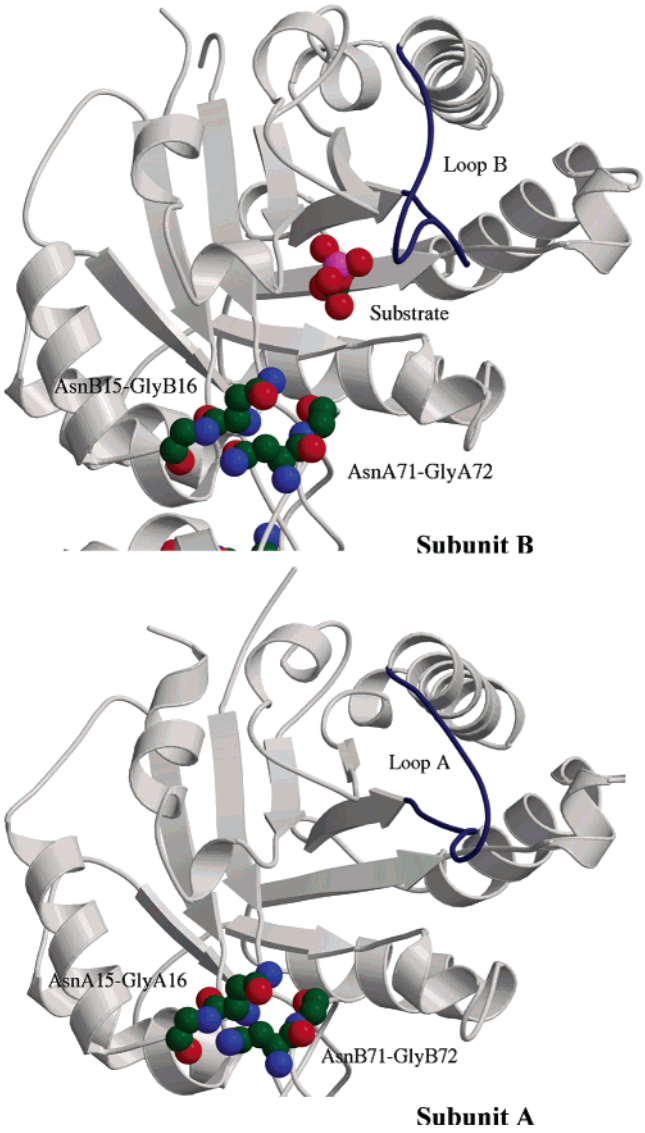

Figure 1. Triosephosphate isomerase enzyme divided into two subunits. On subunit B, the loop is in closed form because of the presence of the substrate; on subunit A, the loop is free to move.

deamidation is largely prevented. At these low water concentrations, TIM exhibits high thermostability due to the decrease in protein flexibility and resistance to hydrolysis of the amide bonds. The data suggest that the rate of deamidation is dependent on the number of catalytic events, on the time that asparagine-71 exists in a conformation favorable for deamidation, and on the solvent environment.

Other studies performed by Gracy et al. have indicated that upon deamidation the enzyme opens, exposing the subunit interface to solvent and thus increasing its proteolytic susceptibility and liability.[25a−d] Their results have also confirmed the fact that the deamidation of Asn_{71} is a prerequisite for the deamidation of the juxtaposed Asn_{15} on the neighboring subunit. Gracy et al. have pointed out the existence of the relationship between the conformational change at the catalytic center and the deamidation process at Asn_{71}-Gly_{72}.[26] This study has been carried out by reacting the active-site Glu_{165} with the substrate analogue CAP, which immobilizes the hinge lid. The CAP-modified homodimers were resistant to deamidation. When the hinged lid on one subunit is immobilized by CAP, the other subunit with the free-hinged lid behaves independently, and deamidation still takes place. The catalytic site is significantly closer to Asn_{71} on the neighboring unit than to Asn_{71} on the same unit. Closing the hinged lid brings the catalytic site much closer to Asn_{71} on the neighboring subunit than to Asn_{71} on the same unit. However, proximity between the catalytic center and the primary deamidation site does not appear to be an essential factor because the two subunits operate independently. Gracy et al. have also stated that although the binding of substrate or CAP to TIM offers initial protection of the enzyme, it appears to distrupt interactions at the subunit interface and to enhance the specific deamidation of Asn_{71} located in the interdigitating loop.[23] This apparent connection between catalysis and deamidation supports the concept of the "molecular wear and tear" mechanism.

The studies done by Capasso et al. have revealed the fact that the deamidation reaction occurs via a succinimide intermediate.[27−28] During deamidation, the β-carbonyl of the asparagine residue acylates the amino group of the next residue, producing an aminosuccinyl residue. This cyclic imide is unstable in aqueous solution, and fast hydrolysis generates either aspartate or isoaspartate peptides in a ratio of 1:3 (Figure 2).[27,29,30] The formation of a succinimide ring has been shown to be a multistep processes with a change in the rate-determining step at around neutral pH,[27] the rate of cyclization being proportional to the pH of the medium.[28] To gain a deeper understanding of the kinetic behavior of this reaction, Capasso et al. have studied the formation of the succinimide derivative from the peptide Ac-Gly-Asn-Gly-Gly-NHMe experimentally. They have proposed a mechanism that explains their kinetic data.[28] At acidic pH, cyclization is the rate-determining step; therefore, the reaction is specific-base-catalyzed. At higher pH, deamidation becomes rate-determining; therefore, the reaction is general-acid−specific-base catalyzed. A significant change in local protein structure is required for the formation of a cyclic imide according to the mechanism explained above; therefore, Gly and to a lesser extent serine (Ser), owing to their small side chains, are more tolerant of this structural change. The reaction mechanism is also consistent with the fact that glutamine (Gln) residues deamidate more slowly than Asn because the formation of a six-membered cyclic imide is entropically less favored.

In our previous theoretical work, the deamidation mechanism suggested by Capasso et al. (Figure 2) has been modeled in vacuum using density functional theory (B3LYP/6-31G*).[31] It has been found that in a basic medium the deamidation process has a higher activation barrier than the cyclization step, in agreement with experimental findings. The hydrolysis of two amide bonds has qualitatively explained the relative experimental ratio (1:3)[27,29,30] of the aspartate versus the isoaspartate product.[31] The results were also consistent with Wright's claim concerning the relative half-lives of hydrolysis versus deamidation,[15] showing that deamidation has a much shorter half-life. The hydrolysis of the succinimide ring has been modeled using density functional theory (B3LYP/6-31+G*) both in neutral and alkali media.[32,33]

In this study, we have investigated the deamidation reaction that takes place on the subunit interface of triosephosphate isomerase by using QM/MM methodology. Our main aim has been to determine whether ligand-induced deamidation occurs via an intrasubunit or intersubunit transmission of the conformational change. QM/MM methodology enables us to describe the deamidating site by quantum mechanics, the rest of the enzyme and the solvating water molecules being described by molecular mechanics.

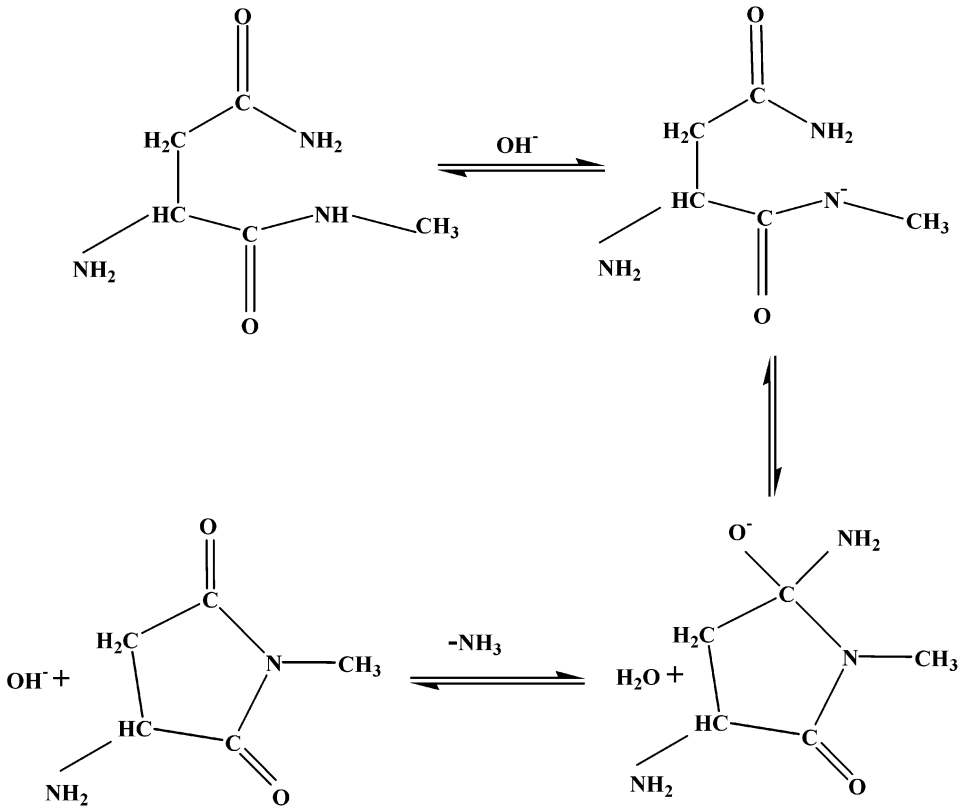

Figure 2. Deamidation mechanism suggested by Capasso et al.

Computational Methods

In 1976, Warshel and Levitt published the first article that describes the basic QM/MM approach.[34] The system of interest is partitioned into two subsystems: one (QM) contains a small number of atoms and is described by quantum mechanics, and the other (MM) represents the rest of the system and is described by a suitable classical force field. The Hamiltonian of the whole system can be written as follows:

$$H = H_{QM} + H_{MM} + H_{QM/MM} \quad (1)$$

The first term is a QM Hamiltonian, the second term is an empirical force field, and the last term is the Hamiltonian that describes the interactions between the QM and MM regions. The total energy of the system can likewise be written as

$$E = E_{QM} + E_{MM} + E_{QM/MM} \quad (2)$$

In principle, many levels of accuracy can be used for the QM region. However, semiempirical approaches are often used in enzymatic catalysis because the QM region is usually of considerable size.

The main problem arising with QM/MM methods is the description of the QM/MM frontier, especially when considering protein structures where atoms located at the border between the two QM and MM regions are linked by covalent bonds. These so-called frontier bonds must be described at the quantum level in order to reproduce their behavior as if the whole system had been included in the quantum computation. Several methods have been suggested to solve the problem.[35] In the local self-consistent field (LSCF),[36−38] the frontier bonds are described by strictly localized bond orbitals (SLBOs) whose characteristics are considered to be constant over the whole reaction process. These SLBOs are frozen in the SCF procedure, which is carried out using a basis set of orbitals orthogonal to the SLBOs in order to generate the molecular orbitals describing the quantum subsystem.

In this study, LSCF semiempirical computations have been performed using the GEOMOP program[39−41] at the NDDO level with AM1 parametrization.[42,43] The electrostatic interactions between the quantum and the classical subsystems (point charges) are included in the electronic Hamiltonian. The classical AMBER force field has been used for the MM part.[44] Intermediates and transition structures along the reaction path have been located by varying the coordinates of the atoms entering the quantum subsystem (i.e., the MM atoms are kept fixed during the location of stationary points). Transition structures have been located using Schlegel's algorithm.[45] They have been characterized with one imaginary frequency. Reaction intermediates connecting the transition structures were determined by following the transition vector on both sides, using the IRC formalism,[46,47] and then by full geometry optimization.

Preparation of the System. The preparation of the initial 3D structure of triosephosphate isomerase (TIM) has been carried out according to the following procedure:

-To understand the effect that the binding site has on the deamidation reaction, the catalytic sites (loop) on the two subunits have been modeled differently: in one subunit, the catalytic site is empty (open form), whereas in the other subunit it is bonded to the CAP substrate (closed form) (Figure 1).

-The initial atomic coordinates of the enzyme are obtained from the crystallographic structures available in the Protein Data Bank (PDB).[48] The structure from the PDB has been chosen according to the specific requirements of our model. It is known that the deamidation takes place only in the mammalian enzyme.[25,26] It is also known that the closed and open forms of the loop close to the active site of the enzyme may influence the deamidating site. Thus, both the open and closed forms of

SCHEME 1: Definition of the Two Considered Model Systems

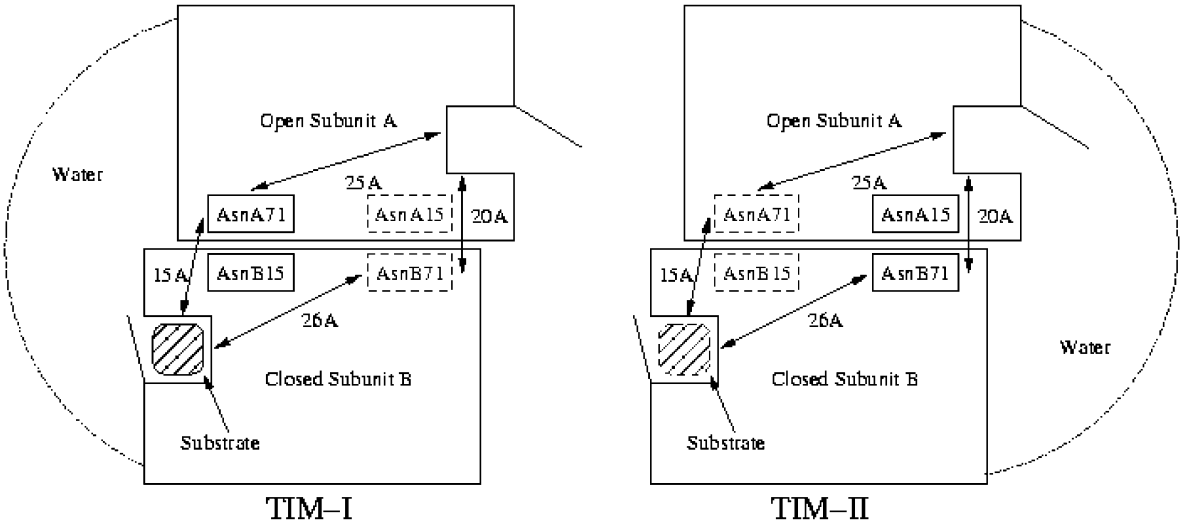

SCHEME 2: Definition of the QM/MM System and the Boundary Atoms in the Enzyme

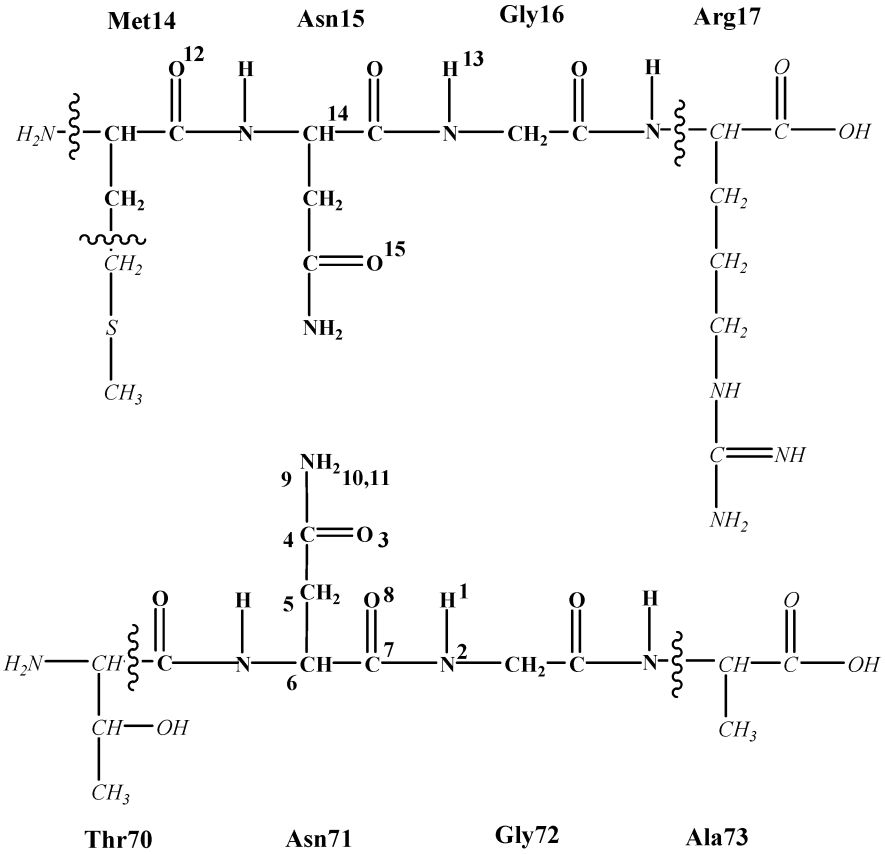

the active site have to be considered along the deamidation reaction. A mammalian PDB structure (entry 1HTI) that has an open loop on subunit A on one side and a closed loop with a substrate analogue on subunit B met our requirements and has been selected.[48] The hydrogen atoms have been added, and the system has been minimized using molecular mechanics.

-The substrate analogue, 2-phosphoglycolic acid (PGA), on subunit B has been changed to 3-chloroacetol phosphate (CAP). It is known from previous studies that when a CAP is bonded to the enzyme the loop motion is prohibited.[26] Thus, the loop on subunit B will be kept closed throughout the study.

-The enzyme must be surrounded by a cap of water molecules in order to simulate its aqueous environment, which is important when mimicking the relationship between deamidation and substrate binding in vivo. However, surrounding the whole enzyme with water molecules is very expensive in terms of computer time. Thus, the following strategy has been adopted. We study two different TIM systems, both built from the same 1HTI dimeric form: in TIM-I, the deamidation sites, Asn_{B15}, and Asn_{A71} have been surrounded by a cap of water molecules. Similarly, in TIM-II, the deamidation sites, Asn_{A15}, and Asn_{B71} have been solvated. TIM-I allows us to model the intersubunit transmission of the conformational change because the catalytic site closest to Asn_{A71} (i.e., the amino acid to be deamidated) is bonded to the substrate and is located on subunit B. Similarly, TIM-II allows us to model the intrasubunit transmission of the

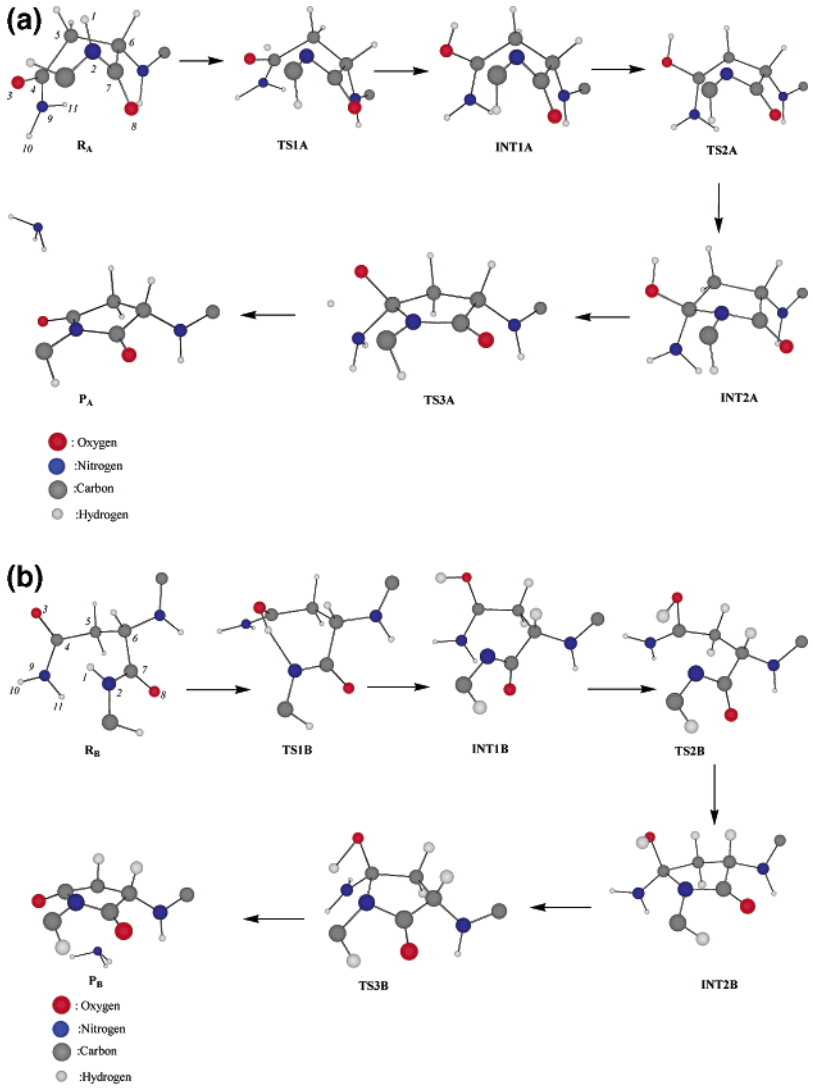

Figure 3. (a) Structural changes obtained at the deamidating site on TIM-I (AsnA71-GlyA72) during the reaction. (b) Structural changes obtained at the deamidating site on TIM-II (AsnB71-GlyB72) during the reaction.

conformational change because the substrate bonded to the catalytic site is on the same subunit B as Asn_{B71} and it is the empty catalytic site on the other subunit that is closer to Asn_{B71}. Only the atoms inside the caps of water are allowed to move during the preparation of the system (Scheme 1).

-The cyclization and deamidation barriers for TIM-I and TIM-II will be evaluated in order to understand how the binding of the enzyme affects deamidation. This is expected to shed light on the relationship between catalysis and deamidation (wear and tear mechanism).

-After an MM optimization of both structures, molecular dynamics runs have been performed with some constraints applied to the systems. To obtain a proper initial geometry for the cyclization step in the deamidation mechanism, a constraint is applied to the C4−N2 distance, which has been allowed to fluctuate between 3.2 and 4.2 Å in the deamidation site (i.e., Asn_{A71} for TIM-I and Asn_{B71} for TIM-II, see Scheme 2). The initial C4−N2 distance was chosen on the basis of the cyclization steps of the model compounds' transition-state geometries. After 150 ps, the constraint on the C4−N2 distance has been removed. The MD calculation has been carried out until 225 ps. The structures having both the smallest C4−N2 distance and a proper dihedral angle for proton transfer have been selected as plausible starting structures for TIM-I and TIM-II.

-Each structure has been partitioned into two parts: QM and MM. In the quantum part, the Met_{14}, Asn_{15}, Gly_{16}, Arg_{17}, Thr_{70}, Asn_{71}, Gly_{72}, and Ala_{73} residues have been chosen. The QM/MM boundaries were between Met_{14} C_α and N, $Met_{14}C_\beta$ and C_γ, Arg_{17} N and C_α, Thr_{70} C_α and C_β, and Ala_{73} N and C_α as shown in Scheme 2. The rest of the enzyme and water molecules were described by means of the classical AMBER force field.[43]

Results

Cyclization and Deamidation Mechanism. The cyclization and subsequent deamidation reaction mechanisms include a series of intermediate and transition states. The 3D structures for the TIM-I and TIM-II systems are shown in Figure 3a and b, respectively. The reaction paths corresponding to the TIM-I and TIM-II systems are displayed in Figure 4a and b, respectively. The main geometrical parameters concerning the stationary structures along the reaction path can be found in Table 1. The two considered model systems are displayed in Scheme 1. The QM/MM system and the boundary atoms are depicted in Scheme 2.

TIM-I. The first step of the reaction path is cyclization. The cyclization reaction is followed by a deamidation reaction. In the TIM-I system, the cyclization reaction is stepwise as opposed to the model reaction.[31] In other words, no transition state has

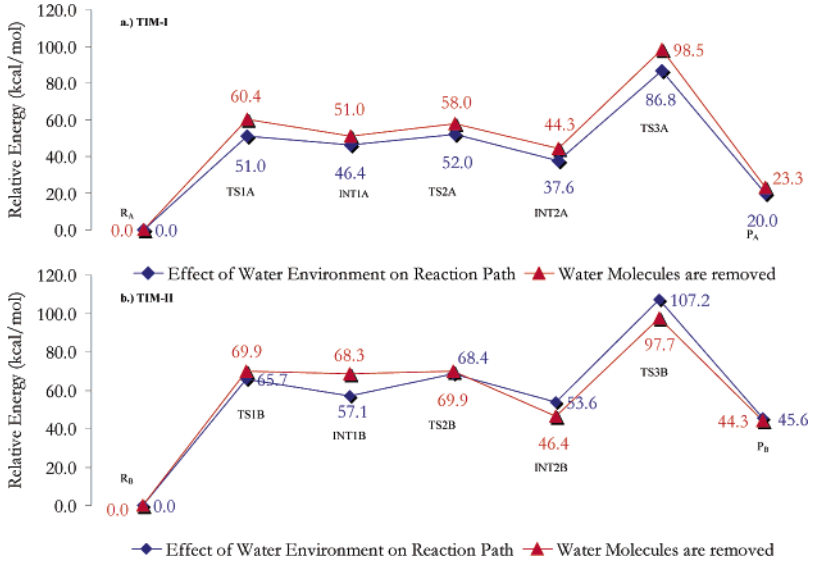

Figure 4. (a) Energy profile obtained for the TIM-I system. (b) Energy profile obtained for the TIM-II system.

been located that would correspond to the concerted hydrogen transfer and C−N bond formation when the system is surrounded by water molecules. First, the proton migrates to a carbonyl oxygen atom. Then, the C−N bond is formed, and the ring is closed (Figure 3a). The side chain of Asn_{A71} can attain an appropriate conformation by rotating the amide group for the proton transfer to occur. This rotation is possible only for a TIM-I system in which the contact in the subunit interface is loosened because of substrate binding on the juxtaposed subunit. In the initial structure R_A, the N2−H1−O3 angle is 17.9°. The distance between H1 and O3 is 3.237 Å. R_A is stabilized by hydrogen bonds and long-range stabilizing interactions. The H1−O15 (2.377 Å) and the H1−O12 distances (2.622 Å) can be visualized as plausible hydrogen bond interactions. The long-range interactions are not limited to the juxtaposed subunit, but water molecules surrounding the enzyme also have a stabilizing effect on the overall mechanism. The transition state TS1A has an activation energy barrier of 51.0 kcal/mol (Figure 4a). The reaction is endothermic, and the geometrical parameters of the transition state are closer to those of the product, in agreement with Hammond's postulate. The elongation of C7−O8 (1.244 to 1.262 Å) and the shortening of N2−C7 (1.384 to 1.356 Å) bonds are strong evidence for the formation of an iminelike structure that stabilizes the transition state. The stabilizing effect due to the formation of this iminelike structure lowers the activation barrier for the proton-transfer reaction. By following the eigenvector of TS1A relative to the imaginary frequency, an intermediate INT1A is located in which the H1 hydrogen atom is completely transferred to the Asn side chain carbonyl (Figure 3a). There is a stabilizing effect arising from interactions between the transferred proton (H1) and O15 (1.898 Å) on the juxtaposed subunit. The final step of the cyclization reaction is the ring closure through the formation of the N2−C4 bond (intermediate INT2A). The corresponding transition state (TS2A) is characterized by one imaginary frequency that basically involves the N2−C4 bond. The reaction step is exothermic. The energy barrier is 5.6 kcal/mol (Figure 4a). Note that the ring is not planar, the nitrogen atom N2 still exhibiting a pyramidal conformation.

The next step is deamidation in which the amine departs from the cyclic intermediate and the planar succinimide ring is formed. The proton transfer (H1) to NH_2 is coupled with the complete breaking of the C2−N7 bond. This concerted deamidation reaction is exothermic, as in the model compound.[31] The activation barrier is 49.2 kcal/mol (Figure 4a).

TIM-II. The initial reactant structure is denoted as R_B. Figure 4b represents the energy profile for the cyclization and deamidation reactions of the Asn_{B71}-Gly_{B72} dipeptide. Water molecules W_{659}, W_{634}, and W_{690} are removed from the system to prevent a plausible collision between $-NH_3$ (leaving group on succinimide) and these molecules. Structure R_B is stabilized by various intermolecular interactions between the amino acids of two juxtaposed subunits at the subunit interface. The distances between H10 and O15 (2.267 Å), H11 and O15 (2.864 Å), and H1 and the oxygen of Met_{14} (O12) on the juxtaposed subunit (2.000 Å) illustrate these stabilizing interactions. In principle, the cyclization step of the deamidation reaction can be either stepwise or concerted, as pointed out above. However, as in the case of TIM-I, our computations predict a stepwise mechanism only. According to this mechanism, the proton (H1) on the nitrogen of glycine is initially transferred to the carbonyl oxygen (O3) of the asparagine side chain. Then ring closure is observed with a nucleophilic attack of N2 to C4. The transition state, TS1B, is characterized by one imaginary frequency that includes the H1, N2, and O3 atoms (Figure 3b). The first step of the cyclization reaction is the rate-determining step having an activation energy of 65.7 kcal/mol. This reaction is highly endothermic. The transition state resembles the product, as in TIM-I. Because of the transfer of H1 on N2, the peptide bond between Asn_{71} and Gly_{72} is distorted. The formation of an iminelike structure on this peptide bond stabilizes TS1B, as in TIM-I. On the basis of the delocalization of the electrons from the carbonyl bond toward the C4−N2 bond, the C7O8 bond distance lengthens (1.270 Å) whereas the N2C7 bond distance shortens (1.337 Å) relative to the reactant (R_B). When the eigenvector of TS1B is followed, an intermediate (INT1B) is obtained in which the H1 atom has been completely transferred to the carbonyl of the asparagine side chain. Hydrogen-bond stabilizing interactions are also present between the transferred proton (H1) and O15 (1.940 Å) and H10 and O15 (2.163 Å).

The next step is the formation of cyclic intermediate INT2B via a nucleophilic attack of the nitrogen to the carbonyl carbon atom (Figure 3b). This reaction is slightly exothermic. The activation energy is 11.2 kcal/mol. Again, because of the presence of the sp^3 carbon atom adjacent to the nitrogen, the ring is not planar. Note that the distance between the sp^3 carbon

TABLE 1: Main Geometrical Parameters Obtained from the TIM-I and TIM-II Systems for the Stationary Points

	R_A	R_B	TS1A	TS1B	INT1A	INT1B	TS2A	TS2B	INT2A	INT2B	TS3A	TS3B	P_B	P_A
C4N2	3.237	3.220	2.982	2.799	2.813	2.868	2.085	2.085	1.536	1.523	1.492	1.501	1.435	1.428
C4O3	1.250	1.259	1.307	1.335	1.336	1.343	1.352	1.362	1.405	1.410	1.339	1.337	1.228	1.227
O3H1	3.239	3.531	1.128	1.069	1.001	0.991	0.980	0.986	0.970	0.974	1.417	1.417	2.919	4.493
N2H1	1.002	1.001	1.586	1.739	2.569	3.779	2.825	2.477	2.783	2.370	2.987	2.984	4.701	5.729
N2C7	1.384	1.367	1.356	1.337	1.340	1.328	1.365	1.359	1.407	1.392	1.383	1.397	1.408	1.428
C7O8	1.244	1.254	1.262	1.270	1.269	1.285	1.252	1.256	1.235	1.239	1.238	1.241	1.233	1.236
N9C4	1.375	1.358	1.345	1.321	1.337	1.324	1.369	1.357	1.462	1.443	1.542	1.536	4.395	4.327
N9H1	4.710	3.018	3.191	2.904	3.102	2.477	3.099	2.645	3.077	2.768	1.317	1.310	1.003	1.001
H1...O12	2.377	1.999	2.979	2.068	4.713	3.951	4.307	2.221	4.084	2.165	4.130	4.637	4.335	6.781
H1...O15	2.622	2.966	2.128	2.835	1.898	1.940	1.946	2.044	1.968	2.059	1.857	2.226	2.344	8.633
N2H1O3	17.9	113.4	22.0	134.4	62.4	114.3	87.6	86.5	101.9	79.4	100.6	54.7		
C4O3H1	21.4	55.3	39.2	108.3	111.0	109.1	109.7	109.3	108.7	107.3	46.0	94.9		
C4O3H1N2	−93.2	12.2	18.1	−10.9	51.2	−0.2	68.7	23.7	84.6	21.5	−117.7	30.1		
O3H12N9C4	45.6	27.9	137.6	70.8	160.5	56.5	−179.6	39.9	−120.2	58.2	1.2	6.9		
C4O3H1N9	156.6	−36.5	162.1	−32.5	171.4	−31.5	−179.3	−28.3	−151.1	−37.1	1.1	−7.9		
C4C5C6C7	−47.1	72.7	−59.0	56.8	−45.6	61.6	−22.4	43.3	−6.8	33.9	9.0	18.1	4.7	21.6
C5C6C7N2	−57.0	−89.9	−18.0	−76.7	−34.7	−73.6	−26.3	−60.7	−20.2	−36.3	−10.0	−31.1	−15.2	−27.9
N2C4C5C6	54.0	−30.9	56.3	−24.3	53.8	−24.5	42.2	−17.7	28.6	−22.3	−4.7	−1.4	6.7	−9.8
C4N2C7C6	62.9	−44.0	39.7	43.8	51.2	42.5	46.6	42.3	39.2	22.5	8.5	31.1	20.2	22.9
C5C4N2C7	−75.9	−7.0	−18.0	−11.8	−68.3	−10.6	−54.6	−15.1	−41.4	0.2	−2.3	−18.1	−16.8	−7.9

atom (C4) and the nitrogen is 0.13 Å longer than the distance between the sp^2 carbon atom (C7) and the same nitrogen.

The deamidation reaction constitutes the final step of the overall mechanism. The reaction is concerted, as in the model compound and TIM-I. The transfer of a proton (H1) to $-NH_2$ and the $-NH_3$ group leaving the system occur simultaneously. At the transition state, the C4 carbon has still sp^3 character. The energy of activation is 53.6 kcal/mol. This reaction is exothermic. After the departure of the $-NH_3$ group, the succinimide ring is formed. The ring is unstable and susceptible to hydrolysis with the formation of either aspartate or isoaspartate.

Discussion

The comparison of the processes with TIM-I and TIM-II shows some common trends. For both systems, the stepwise cyclization process is initiated by a proton transfer that requires a substantial amount of activation energy. Ring closure following this proton transfer is relatively easy. After cyclization, deamidation takes place, the corresponding activation barrier being rather large.

Though the TIM-I and TIM-II systems exhibit the same qualitative reaction mechanisms, some important differences are found when one compares the energy profiles. First, it may be noted that all of the structures described along the reaction path are much less stable (relative to the corresponding reactant) for the reaction with TIM-II. In particular, the highest TS along the energy profile with TIM-II (TS3B) is about 20 kcal/mol higher than the corresponding transition-state structure in the TIM-I profile (TS3A). Similarly, the product PB is less stable than PA by about 25 kcal/mol, showing that although both reaction mechanisms are endothermic TIM-II deamidation is much more unfavorable from a thermodynamic point of view.

A comparison of the energetic values of the model dipeptide in vacuum reported before[31] and those obtained here for TIM-II shows that the environment alters not only the nature of the cyclization step but also the heats of reaction. The cyclization step in vacuum computed either with AM1 or B3LYP/6-31G* is a concerted mechanism, whereas in TIM-I or in TIM-II this is a stepwise mechanism. The energy barriers are respectively 62.5 and 54.5 kcal/mol for AM1 and B3LYP/6-31G* in vacuum. The second step of the reaction deamidation is a concerted mechanism both in vacuum and in TIM. The energy barriers are respectively 48.3 kcal/mol with AM1 in vacuum, 33.2 kcal/mol with B3LYP/6-31G* in vacuum, 49.2 kcal/mol with AM1 in TIM-I, and 53.6 kcal/mol with AM1 in TIM-II. Overall, although AM1 overestimates energy barriers as compared to DFT calculations in vacuum, qualitative agreement is reached in vacuum for the reaction mechanism (i.e., concerted cyclization and concerted deamidation steps, the highest barrier corresponding to the cyclization step). This enables us to have relatively good confidence in our results in TIM-I and TIM-II, namely, a stepwise cyclization step and a concerted deamidation step, the highest barrier corresponding to the cyclization step.

In line with the experimental findings stating that the deamidation does not often occur, the deamidation reaction that we have here has a high barrier (~50 kcal/mol). This is in agreement with the fact that the rate of deamidation is dependent not only on the number of catalytic events but also on the time that asparagine-71 exists in a suitable conformation as well as on the presence of a favorable solvent environment.[24] Otherwise, the enzyme would have a short lifetime.

To analyze the energetic contribution of the water molecules, we removed these molecules and recomputed the energy profiles

TABLE 2: Energetic Contributions to the Total Energy along the Reaction Path of the Total MM Part and Some Selected Residues Described Classically (kcal/mol)

TIM-I	R_A	TS1A	INT1A	TS2A	INT2A	TS3A	P_A
full MM environment	−62.2	−55.0	−56.6	−60.4	−60.4	−53.2	−65.6
TIM+CAP	−47.8	−46.0	−45.5	−50.0	−51.6	−49.3	−51.5
water	−14.4	−8.9	−11.1	−10.4	−8.8	−3.9	−14.1
CAP	−4.1	−1.9	−1.8	−4.8	−7.4	−6.6	−7.1
loop A	−0.3	−0.4	−0.5	−0.4	−0.3	−0.4	−0.3
loop B	0.5	0.6	0.8	0.9	0.9	1.1	0.9
Phe_{A74}	−6.9	−7.4	−7.3	−7.2	−6.9	−6.9	−6.9
Ser_{A79}	−6.2	−6.5	−6.5	−6.6	−6.2	−6.4	−5.7
Gly_{A81}	−2.4	−2.4	−2.5	−2.6	−2.6	−2.6	−2.4
Met_{A82}	−7.3	−7.4	−7.2	−7.4	−7.5	−7.9	−7.8
Lys_{A84}	−5.2	−4.0	−4.8	−5.7	−6.1	−6.1	−6.3
Trp_{B12}	−7.4	−5.8	−5.3	−7.7	−7.7	−6.5	−7.4
Ser_{B20}	−3.1	−2.8	−2.9	−3.0	−3.1	−2.9	−3.5
Asp_{A49}	1.7	1.6	2.0	2.0	1.9	2.2	2.3
Val_{A69}	3.1	2.5	3.1	3.1	2.4	3.4	2.6
Asp_{A85}	3.5	2.8	3.5	3.8	3.9	4.3	4.8
Glu_{A104}	1.1	2.0	2.3	1.9	1.4	1.8	1.2
Glu_{A119}	3.0	1.8	2.3	4.2	4.7	4.4	4.2
Lys_{B13}	2.0	−0.1	−0.8	1.1	3.7	2.0	3.5
TIM-II	R_B	TS1B	INT1B	TS2B	INT2B	TS3B	P_B
full MM environment	−21.0	−12.1	−17.1	−9.3	−0.8	−2.7	−8.5
TIM+CAP	−6.2	9.1	6.6	5.7	6.2	6.1	6.1
water	−14.8	−21.1	−23.8	−15.1	−7.0	−8.8	−14.6
CAP	1.6	2.1	2.1	1.9	1.6	1.9	1.7
loop A	0.8	0.4	0.5	0.6	0.7	0.5	0.5
loop B	−0.4	−0.6	−0.6	−0.5	−0.4	−0.5	−0.4
Phe_{B74}	−6.8	−6.6	−6.3	−7.4	−7.2	−6.8	−6.8
Ser_{B79}	−6.1	−7.3	−7.5	−6.9	−6.4	−5.8	−5.3
Gly_{B81}	−4.3	−4.3	−4.4	−4.3	−4.1	−4.0	−3.9
Met_{B82}	−6.9	−6.6	−6.5	−6.4	−6.4	−6.7	−6.4
Lys_{B84}	−10.0	−8.3	−9.0	−9.1	−9.4	−8.6	−8.9
Trp_{A12}	−7.4	−8.6	−9.1	−8.6	−8.3	−7.2	−6.2
Lys_{A18}	−5.8	−4.1	−4.5	−4.4	−4.7	−5.3	−5.1
Asp_{B49}	3.3	2.3	2.5	2.4	2.5	3.2	2.9
Asp_{B85}	7.1	4.1	4.7	4.6	5.2	6.0	5.8
Glu_{B104}	1.7	3.1	3.1	2.7	2.1	2.3	2.0
Glu_{B119}	8.9	7.9	8.6	8.7	8.7	7.4	8.0
Lys_{A13}	12.0	10.8	10.5	13.1	14.1	10.5	9.5
Lys_{A237}	3.5	4.9	4.9	4.3	3.4	3.7	3.4

by using single-point energy calculations. The results are presented in Figure 4. For the TIM-I system, the presence of a water environment is the driving force for the reaction, all of the structures along the process being stabilized with respect to the reactants. When the water molecules are removed, the energy barrier of the proton-transfer reaction is increased by about 10 kcal/mol, and the deamidation barrier (TS3A−INT2A) increases by about 5 kcal/mol (Figure 4a). The result for TIM-II is relatively surprising. Solvation plays a stabilizing role in the first part of the process only, up to TS2B, but destabilizes all of the structures beyond it. Removing water molecules produces a destabilizing effect of about 5 kcal/mol in the first step, whereas the deamidation barrier (TS3B−INT2B) decreases by about 2 kcal/mol.

In terms of energy barriers, the deamidation reaction can be decomposed in two main barriers: $R_{A/B} \rightarrow TS1_{A/B}$ (proton transfer) and $INT2_{A/B} \rightarrow TS3_{A/B}$ (deamidation step). Both barriers are lower for TIM-I as compared to TIM-II: 51.0 kcal/mol for $R_A \rightarrow TS1_A$ and 49.2 kcal/mol for $INT2_A \rightarrow TS3_A$ vs 65.7 kcal/mol for $R_B \rightarrow TS1_B$ and 53.6 kcal/mol for $INT2_B \rightarrow TS3_B$. Moreover, the kinetics of the reverse reaction (from products to reactants) is more unfavored in the case of TIM-I than in the case of TIM-II. The main reverse-reaction barrier is 66.8 kcal/mol for TIM-I versus 62.8 kcal/mol for TIM-II. This again strengthens the idea that the deamidation reaction is much more favored when the substrate is in the vicinity of the deamidation site (TIM-I model) rather than when there is no substrate around it (TIM-II model). Overall, the CAP substrate acts as a catalyst for the deamidation reaction in triose phosphate isomerase: it speeds up the kinetics of the reaction without being thermodynamically a part of it.

The contribution of individual residues to the total energy can also be computed by $\langle\psi|H_i^{QM/MM}|\psi\rangle$, where ψ is the polarized wave function and $H_i^{QM/MM}$ represents the perturbation due to residue i. The positive values come from the destabilizing interactions between the QM and MM parts, whereas negative values indicate the stabilizing interactions between them. In Table 2, the individual contributions of some residues and of the whole MM part are considered. It appears that the MM environment has a global stabilizing influence on the reaction in TIM-I. Among the most stabilizing amino acids, one can find Phe_{A74}, Ser_{A79}, Met_{A82}, Lys_{A84}, Trp_{B12}, and so forth. The CAP substrate is part of the stabilizing effect of the deamidation reaction in TIM-I. Most destabilizing amino acids in TIM-I are negative amino acids close to the deamidation site (Asp_{A49}, Glu_{A77}, Asp_{A85}, Glu_{A104}, Glu_{A119}). Lys_{B13} also has a destabilizing influence on the deamidation reaction in TIM-I. In TIM-II, with the exception of R_B, the effect of the MM environment is mainly a destabilizing effect. Water gives a negative contribution to the total energy in the same range as in TIM-I. CAP, which is quite far away from the TIM-II deamidation site, now has a destabilizing influence on the TIM-II reaction pathway. Like their equivalent in TIM-I, Phe_{B74}, Ser_{B79}, Met_{B82}, Lys_{B84}, and Trp_{B12} have also strong negative energetic contributions to the

total energy along the TIM-II reaction path. The close, negatively charged amino acids have in TIM-II a destabilizing effect, but this effect is much more important than in TIM-I, especially with Lys13 (around +12 kcal/mol along the TIM-II reaction path instead of about +2 kcal/mol for TIM-I). In both systems, the effect of the loop does not seem to be significant. Overall, it is the protein that has the most important influence on the reactivity. In TIM-I, the deamidation reactivity is favored as compared to the situation in TIM-II.

There are experimental results indicating that Lys_{13} plays a role during the binding of the substrate to the catalytically active site of the enzyme.[13] The positive charges on the side chain of Lys_{13} interact with the negatively charged substrate and should in principle stabilize the catalytic site. It is important to note that the contribution of Lys_{13} (Lys_{13} on subunit B) is more important in TIM-II and that its effect is a destabilizing one.

There is strong evidence for the relationship between the hydrogen bond network present in the enzyme and the reactivity differences between the two subunits. Indeed, when the crystallographic data is studied, the importance of the hydrogen bond network becomes evident. Although the binding of the substrate to one subunit strengthens the intrasubunit hydrogen bond network, it weakens the intersubunit one. In TIM-I, strong interaction between the Lys_{B13} and phosphate oxygens of CAP is observed. When substrate binds to enzyme, the phosphate oxygens interact with the side-chain $-NH_3$ of Lys_{B13} (1.68 Å). The same lysine residue strengthens its interaction with His_{B95} (3.68−2.72 Å). When Lys_{B13} is pulled out by these residues, Asn_{B15} moves toward it. The distance between Asn_{A15} (H) and Lys_{A13} (O) is 1.75 Å in TIM-I and 1.87 Å in TIM-II. Another stronger interaction between the side chains of Asn_{A15} (H) and Lys_{A13} (O) is identified (3.07 Å) for TIM-I. Increases in the distances between $Asn_{B15}-Asn_{A71}$ (2.77 vs 3.03 Å), Met_{B14}-Gly_{A72} (2.82 vs 2.96 Å), and $Arg_{B17}-Asn_{A71}$ (2.62 vs 2.89 Å) can be attributed to the weakening of the intersubunit interactions in the TIM-I system as compared to that in TIM-II. The distances obtained from the molecular dynamics run are in accordance with the crystallographic data. Thus, the binding of the substrate provides a space at the subunit interface that allows the side chain of asparagines to make proper conformational changes in order to initiate the deamidation reaction. The deamidation priority of Asn_{71} can be explained with this point of view. The enhancement of the intrasubunit hydrogen bond network through substrate binding prevents the deamidation of Asn_{15}, whereas it enables the deamidation of Asn_{71}. Hence, it can be concluded that the ligand-induced deamidation reaction on triosephosphate isomerase occurs via an intersubunit transmission of the conformational change, the binding of substrate modifying the conformational preferences of the Asn_{15} on the same subunit. The overall effect can be described as an intersubunit mechanism because deamidation takes place on the juxtaposed subunit.

Conclusions

The energetic comparison of the TIM-I and TIM-II systems and geometrical parameters obtained after the MD runs enable us to derive some conclusions about the relationship between the deamidating site and the catalytic activity of the enzyme.

In TIM-I, the cyclization and deamidation steps are competing. The activation barrier for the cyclization step is 2 kcal/mol higher than for the deamidation step. In TIM-II, the difference is 12 kcal/mol. In experimental studies, Capasso et al. have found that at acidic pH the cyclization is the rate-determining step for hexapeptides. In our case, although the medium is neutral, the rate-determining step is cyclization in both systems.

The formation of an intramolecular hydrogen bond network on one subunit during the binding of the substrate on the same subunit prohibits the deamidation of Asn_{15} on the same subunit. Our results confirm the experimental results found by Gracy et al. After the deamidation of Asn_{71} on one subunit, Asn_{15} on the juxtaposed subunit will take the proper conformation to initiate the deamidation reaction. Gracy et al. have also stated that the binding of the substrate or CAP to TIM spoils the hydrogen bond network at the subunit interface, enhancing the specific deamidation of Asn_{71} located in the interdigitating loop.[25] Our results also confirm that the conformational changes that stem from the substrate binding on one subunit allow the deamidation reaction on the juxtaposed subunit. These calculations suggest a possible answer to the crucial question on the relationship between the deamidation reaction and the catalytic activity of the enzyme triosephosphate isomerase.

Acknowledgment. This project was initiated upon the request of Dr. U. Yuksel, who has experimentally analyzed the deamidation reaction of the enzyme triosephosphate isomerase (TIM). We appreciate his efforts and suggestions. We thank Dr. B. Maigret for fruitful discussions. We acknowledge the financial support of Tubitak-CNRS (project no.297) and Boğaziçi University Araştırma Fonu. F.A.S.K. thanks the members of the Laboratoire de Chimie Theorique for their hospitality and support during her visit to Nancy. F.A.S.K is grateful to BUVAK and the Department of Chemistry at Boğaziçi University for financial support.

References and Notes

(1) Knowles, J. R. *Nature* **1991**, *350*, 121.
(2) Blacklow, S. C.; Raines, R. T.; Lim, W. A.; Zamore, P. A.; Knowles, J. R. *Biochemistry* **1998**, *27*, 1158.
(3) Alberly, W. J.; Knowles, J. R. *Biochemistry* **1976**, *15*, 5588−5600.
(4) Lollis, E.; Petsko, G. A. *Biochemistry* **1990**, *29*, 6619−6625.
(5) Wierenga, R. K.; Noble, M. E. M.; Davenport, R. C. *J. Mol. Biol.* **1992**, *224*, 1125−1126.
(6) Cui, Q.; Karplus, M. *J. Am. Chem. Soc.* **2001**, *123*, 2284−2290.
(7) Cui, Q.; Karplus, M. *J. Phys. Chem. B* **2002**, ASAP article.
(8) Joseph, D.; Petsko, G. A.; Karplus, M. *Science* **1990**, *249*, 1425−1428.
(9) Pompliano, D. L.; Peyman, A.; Knowles, J R. *Biochemistry* **1990**, *29*, 3186−3194.
(10) Schanekerz, K. D.; Kuan, T. K.; Goux, W. J.; Gracy, R. W. *Biochem. Biophys. Res. Commun.* **1990**, *173*, 736−740.
(11) Derreumaux, P.; Schlick T. *Biophys. J.* **1998**, *74*, 72−81.
(12) (a) Bash, P. A.; Field, M. J.; Davenport, R. C.; Petsko, G. A.; Ringe, D.; Karplus, M. *Biochemistry* **1991**, *30*, 5826−5832. (b) Karplus, M.; Evanseck, J. D.; Joseph, D.; Bash, P. A.; Field, M. J. *Faraday Discuss.* **1992**, *93*, 239−248.
(13) Lodi, P. J.; Chang, L. C.; Knowles, J: R.; Komives, E. A. *Biochemistry* **1994**, *33*, 2809−2814.
(14) Neria, E.; Karplus, M. *Chem. Phys. Lett.* **1997**, *267*, 23−30.
(15) Wright, H. T. *CRC Crit. Rev. Biochem.* **1991**, *26*, 1−52
(16) Gracy, R. W.; Yuksel, K. U.; Jacobson, T. M.; Chapman, M. L.; Hevelone, J. C.; Wise, G. E.; Dimitrijevich, S. *Gerontology* **1991**, *37*, 113−127.
(17) Bischoff, R.; Kolbe, H. V. J. *J. Chromatogr., B* **1994**, *662*, 261−278.
(18) Robinson, A. B.; Rudd, C. *Curr. Top. Cell Regul.* **1974**, *8*, 247−295.
(19) Johnson, B. A.; Aswad, D. W. In *Deamidation and Isoaspartate Formation in Peptides and Proteins*; Aswad D. W., Ed.; CRC Press: Boca Raton, FL, 1995.
(20) Tang, C. Y.; Yuksel, K. U.; Jacobson, T. M.; Gracy, R. W. *Arch. Biochem. Biophys.* **1990**, *283*, 12−19.
(21) Yuan, P. M.; Talent, J. M.; Gracy, R. W. *Mech. Ageing Dev.* **1981**, *17*, 151−162.
(22) Gracy, K. N.; Yuksel, K. U.; Gracy, R. W. *Mech. Ageing Dev.* **1990**, *56*, 179−186.
(23) Sun, A−Q.; Yuksel, K. U.; Gracy, R. W. *Arch. Biochem. Biophys.* **1992**, *293*, 382−390.
(24) Ramos-Garza, G.; Gomez-Poyou, M. T.; Gomez-Poyou, A.; Yuksel, K. U.; Gracy, R. W. *Biochemistry* **1994**, *33*, 6960−6965.

(25) (a) Sun, A.-Q.; Yuksel, K. U.; Gracy, R. W. *J. Biol. Chem*. **1995**, *322*, 361−368. (b) Sun, A.-Q.; Yuksel, K. U.; Rao, G. S. J.; Gracy, R. W. *Arch. Biochem. Biophys*. **1992**, *295*, 421−428. (c) Sun, A.-Q.; Yuksel, K. U.; Gracy, R. W. *J. Biol. Chem*. **1992**, *267*, 20168−20174. (d) Gracy, R. W.; Talent, J. M.; Zvaigzne, A. I. *J. Exp. Zool*. **1998**, *282*, 18−27.

(26) Talent, J. M.; Zvaigzne, A. I.; Agrawal, N. Gracy, R. W. *Arch. Biochem. Biophys.* **1997**, *340*, 1, 27−35.

(27) Capasso, S.; Mazzarella, L.; Sica, F.; Zagon, A. *Pept. Res*. **1989**, *2*, 195−197.

(28) Capasso, S.; Mazzarella, L.; Sica, F.; Zagari, A.; Salvatori, S. *J. Chem. Soc., Perkin. Trans.* **1993**, *2*, 679−682.

(29) Gieger, T.; Clarke, S. *J. Biol. Chem.* **1987**, *262*, 785−794.

(30) Meinwald, C. Y.; Stimson, E. R.; Scherega, H. A. *Int. J. Pept. Protein Res*. **1986**, *28*, 79−84.

(31) Konuklar (Sungur), F. A.; Aviyente, V. A.; Sen. T. Z.; Bahar, I. *J. Mol. Model*. **2001**, *7*, 147−160.

(32) Konuklar, F. A.; Aviyente, V. A.; Ruiz-Lopez, M. F. *J. Phys. Chem. A* **2002**, *106*, 11205−11214.

(33) Konuklar, F. A. S.; Aviyente, V. A. *Org. Biomol. Chem.* **2003**, *1*, 2290−2297.

(34) Warshel, A. Levitt, M. *J. Mol. Biol*. **1976**, *103*, 227−249.

(35) Monard, G.; Merz, K. M., Jr. *Acc. Chem. Res.* **1999**, *32*, 904−911.

(36) Thery, V.; Rinaldi, D.; Rivail, J.-L.; Maigret, B.; Ferenczy, G. G. *J. Comput. Chem*. **1994**, *15*, 269−282.

(37) Monard, G.; Loos, M.; Thery, V.; Banka, K.; Rivail, J.-L. *Int. J. Quantum Chem.* **1996**, *58*, 153−159.

(38) Assfeld, X.; Rivail, J.-L. *Chem. Phys. Lett*. **1996**, *263*, 100−106.

(39) Rinaldi, D.; Hoggan, P. E.; Cartier, A.; Banka, K.; Monard, G.; Loos, M.; Mokrane, A.; Dillet, V.; Thery, V. *GEOMOP*; in press.

(40) Antonczak, S.; Monard, G.; Lopez, M. F.; Rivail, J.-L. *J. Mol. Model.* **2000**, *6*, 527−538.

(41) Reuter, N.; Loos, M.; Monard, G.; Cartier, A.; Maigret, B.; Rivail, J.-L. *Mol. Eng.* **1997**, *7*, 349−365.

(42) Stewart, J. J. P. *J. Comput. Chem.* **1989**, *10*, 209−211.

(43) Merz, K. M., Jr.; Dewar, M. J. S. *Organometallics* **1990**, *7*, 522−524.

(44) Winer, S. J.; Kollman, P. A.; Nguyen, D. T.; Case, D. A. *J. Comput. Chem.* **1986**, *7*, 230−252.

(45) Schlegel, H. B. *J. Comput. Chem.* **1982**, *3*, 214−218.

(46) Gonzales, C.; Schlegel, H. B. *J. Phys. Chem.* **1990**, *90*, 2154−2161.

(47) Beapark, M. J.; Robb, M. A.; Schlegel, H. B. *Chem. Phys. Lett.* **1994**, *223*, 269−272.

(48) Mande, S. C.; Mainfold, V.; Kalk, K. H.; Goraj, K.; Maritial, J. A.; Hol, W. G. *Protein Sci.* **1994**, *3*, 810−821.